Heliyon 10 (2024) e36111

Contents lists available at ScienceDirect

Heliyon

journal homepage: www.cell.com/heliyon

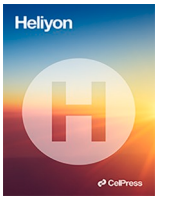

Research article

The contribution of adiponectin to diabetic retinopathy progression: Association with the AGEs-RAGE pathway

Min Fu [a,1], Li Zhengran [a,b,1], Li Yingli [a,1], Wu Tong [a,c], Cai Liyang [a], Guo Xi [d], Yang Xiongyi [a,b], Cao Mingzhe [f,**], Yi Guoguo [e,g,*]

[a] Department of Ophthalmology, Zhujiang Hospital, Southern Medical University, Guangzhou, China
[b] The Second Clinical School, Southern Medical University, Guangzhou, China
[c] The First Clinical School, Southern Medical University, Guangzhou, China
[d] School of Psychological and Cognitive Sciences and Beijing Key Laboratory of Behavior and Mental Health, Peking University, Beijing, China
[e] Department of Ophthalmology, The Sixth Affiliated Hospital, Sun Yat-sen University, Guangzhou, China
[f] Department of Ophthalmology, The Seventh Affiliated Hospital of Sun Yat-Sen University, Shenzhen, 518107, Guangdong Province, China
[g] Biomedical Innovation Center, The Sixth Affiliated Hospital, Sun Yat-sen University, Guangzhou, China

ARTICLE INFO

Keywords:
Eye
Glucose
Genomics
Inflammation
Diabetic retinopathy
Advanced glycation end products
Adiponectin
Single-cell RNA sequencing
ELISA

ABSTRACT

Diabetic retinopathy (DR) is a chronic complication of diabetes. Given that adiponectin plays a key role in DR progression, this study aims to elucidate the molecular mechanisms of sDR progression related to adiponectin. First, we extracted the microarray dataset GSE60436 from the Gene Expression Omnibus (GEO) database to identify hub genes associated with DR. Pathway enrichment analysis revealed a focus on inflammation, oxidative stress, and metabolic disease pathways. Gene Set Enrichment Analysis (GSEA) identified nine significant pathways related to DR. Immune infiltration analysis indicated increased infiltration of fibroblasts and endothelial cells in DR patients. Second, at the gene level, single-cell RNA sequencing (scRNA-seq) results showed a decrease in ADIPOQ gene expression as the disease progressed in our mouse models. At the protein level, ELISA results from sera of 31 patients and 11 control subjects demonstrated significantly lower adiponectin expression in the proliferative diabetic retinopathy (PDR) group compared to controls. Our findings reveal that adiponectin is involved in the advanced glycation end products (AGEs) and receptor of advanced glycation end products (RAGE) axis, as evidenced by hub gene analysis, scRNA-seq, and ELISA. In conclusion, adiponectin acts as a central molecule in the AGEs-RAGE axis, regulated by ADIPOQ, to influence DR progression.

1. Introduction

Diabetes is one of the most serious and critical health problems of the 21st century, leading to a significant increase in the number of adults living with diabetes worldwide, from 108 million to 537 million over the past 40 years [1]. Chronic hyperglycemia can result in

* Corresponding author. Department of Ophthalmology, The Sixth Affiliated Hospital, Sun Yat-sen University, No. 26, Erheng Road, Yuancun, Tianhe, Guangzhou, Guangdong, China.
** Corresponding author. Department of Ophthalmology, The Seventh Affiliated Hospital of Sun Yat-Sen University, Shenzhen, 518107, Guangdong Province, China.
E-mail addresses: caomzh7@mail.sysu.edu.cn (C. Mingzhe), yigg@mail.sysu.edu.cn (Y. Guoguo).
[1] The three authors contributed equally (Co-first authors).

https://doi.org/10.1016/j.heliyon.2024.e36111
Received 7 February 2024; Received in revised form 9 July 2024; Accepted 9 August 2024
Available online 12 August 2024

Abbreviations

DR	Diabetes retinopathy
PDR	Proliferative diabetes retinopathy
NPDR	non-proliferative diabetes retinopathy
scRNA-seq	Single-cell RNA sequencing
ADIPOQ	Adiponectin
STZ	Streptozotocin
AGEs	Advanced glycation end products
RAGE	The receptor of advanced glycation end products
AGER	Advanced glycosylation end product specific receptor
esRAGE	Endogenous secreted receptor of advanced glycation end products
NADPH	Nicotinamide Adenine Dinucleotide Phosphate Oxidase
GEO	Gene Expression Omnibus
DEG	Differentially expressed genes
PPI	Protein-protein interaction
FVMs	Fibrovascular membranes
GO	Gene Ontology
KEGG	Kyoto Encyclopedia of Genes and Genomes
GSEA	Gene Set Enrichment Analysis
VEGF	Vascular endothelial growth factor
HRP	Horseradish peroxidase
FDR	False Discovery Rate
UMAP	Uniform Manifold Approximation and Projection
AMPK	AMP-activated protein kinase
PPARα	Peroxisome proliferator-activated receptor alpha
IRS1	Insulin receptor substrate 1
PI3K	Phosphatidylinositol kinase
HIF-1	hypoxia-inducible factor 1
BP	Biological Process
CC	Cellular Component
MF	Molecular Function

disabling or fatal complications such as diabetic retinopathy (DR), diabetic kidney disease, and cardiovascular diseases [2]. Among these, DR is the primary cause of adult vision loss, with approximately 35 % of diabetic patients exhibiting some degree of DR and 7 % suffering from vision-threatening proliferative DR [3–6]. DR is categorized into proliferative DR (PDR), characterized by the presence of neovascularization in the retina or optic nerve papilla, and non-proliferative DR (NPDR), which lacks these features. As the disease progresses, various risk factors interact, leading to fibrous hyperplasia, vitreous hemorrhage, and retinal detachment, ultimately causing severe vision loss or even complete blindness [7].

AGEs are highly reactive molecules formed and accumulated either endogenously or exogenously due to significantly enhanced non-enzymatic glycosylation of macromolecules (such as proteins and lipids) during prolonged exposure to hyperglycemia [8,9]. The high accumulation of AGEs not only exacerbates oxidative stress by promoting excessive production of reactive oxygen species (ROS) in the retina, leading directly to mitochondrial dysfunction [10], but also stimulates NF-κB signaling and ROS crosstalk, both of which interact to promote inflammation and apoptosis [11]. The intracellular effects of AGEs are mediated through their binding to the receptor for RAGE, a transmembrane receptor and member of the immunoglobulin family. RAGE is encoded by the advanced glycosylation end product-specific receptor (AGER) gene, located in the major histocompatibility complex class III region on chromosome 6p21.3 [12]. The increased expression of RAGE mediates oxidative stress and persistent activation of inflammation, including the NF-κB signaling pathway [13]. RAGE exists in two other forms: a soluble form that circulates in the blood and an alternatively spliced isoform known as endogenous secreted RAGE (esRAGE), which lacks the NF-κB domain and acts as a decoy receptor rather than inducing inflammation [14,15]. These two forms can compete with membrane-bound RAGE, serving as protective factors against inflammation when present in sufficient quantities. The AGEs-RAGE interaction activates signaling proteins and transcription factors, leading to changes in cellular responses that promote the activation of the nicotinamide adenine dinucleotide phosphate (NADPH) oxidase system, resulting in the formation of ROS and consequent cellular oxidative damage [16], as well as microcirculatory changes [17]. Since the formation and accumulation of AGEs occur under hyperglycemic, oxidative stress, and inflammatory conditions, and RAGE expression is enhanced by its ligand AGEs, the AGEs-RAGE interaction may form a positive feedback loop that further promotes the development of diabetes-related microvascular complications.

Research indicates that the interaction of AGEs, a marker of insulin resistance in humans, with RAGE triggers oxidative stress and inflammatory reactions in adipocytes, contributing to insulin resistance [18–20]. An abnormal ADIPOQ pathway, which is significantly associated with RAGE [21], leads to increased insulin resistance [22]. Coincidentally, polymorphisms in ADIPOQ, the gene

encoding adiponectin [23], which has been previously proven to be associated with cardiovascular complications of diabetes [24,25], are now also considered to be related to early DR [26,27]. Adiponectin, secreted almost exclusively by adipocytes, has a protective effect against AGEs-induced endothelial dysfunction and can effectively counteract the dysregulation of AGEs-RAGE axis homeostasis [28]. However, the precise role of ADIPOQ in the regulation of microvascular complications, including DR, and the direct causal relationship between adiponectin and DR, remain unclear. Our study aims to elucidate the molecular mechanisms of early DR progression related to adiponectin. To provide a broader perspective for the early diagnosis and treatment of DR.

To explore the molecular mechanisms involved, we downloaded the original microarray dataset GSE60436 from the GEO database to analyze differentially expressed genes (DEGs). We conducted functional enrichment and constructed a protein-protein interaction (PPI) network to identify genes significantly associated with diabetic retinopathy. Subsequently, we measured adiponectin and PAQR4 concentrations in rats at different disease stages and further investigated the concentrations of key molecules during the same time periods. Using single-cell sequencing, we examined mRNA expression in rat retinal microglia at various disease stages to validate the expression of each key gene. The expression of key genes and proteins was validated by ELISA. We also recruited clinical patients and healthy volunteers, collecting serum samples for ELISA to detect the expression of AGE, RAGE, ADIPOQ, and other related markers. This was done to elucidate their roles in the occurrence and progression of DR. Based on these validation results, we summarized and proposed our hypothesis to provide novel and unique insights into the involvement of adiponectin in the AGEs-RAGE axis-mediated diabetic retinopathy, thereby contributing to the clinical management of diabetic retinopathy.

2. Materials and methods

2.1. Bioinformatics mining

2.1.1. Microarray data

We searched the GEO database for "diabetic retinopathy" (https://www.ncbi.nlm.nih.gov/geo/). We narrowed the search to item type (series), study kind (expression profile by array), and tissue source (*Homo sapiens*), yielding 28 results. The dataset GSE60436 [29] ran on the GPL6884 platform (Illumina HumanWG-6 v3.0 expression beadchip). The study comprised samples from three normal retinal tissues from healthy donors and six fibrovascular membranes (FVMs) from DR patients, three of which were active and the other three inert. We downloaded the platform and series matrix files from GEO and saved them to TXT format. R program (version 4.0.5) was used to process the files.

2.1.2. Data processing and identification of DEGs

We used R to turn the provided platform and series matrix files into an annotation package. The probe name IDs were translated to gene symbols using the R package "hugene10sttranscriptcluster.db" and saved as a TXT file. DEGs were considered significant when the corrected P-value was less than 0.05 and the fold change was more than 1.0. We used the "limma" package [30] to examine DEGs in DR and control samples. A volcano plot generated by the limma package was used to illustrate all up-regulated and down-regulated DEGs, while the top 50 DEGs were visualized using a heatmap created using the Heatmap tool in R software.

2.1.3. GO and KEGG pathway enrichment analyses of significant related genes

We identified 250 DEGs with the lowest P-values and 11 sites associated with AGER as “significant genes.” Functional and pathway enrichment analyses of the proteins encoded by these genes were conducted using R software. We performed Gene Ontology (GO) analysis—encompassing biological processes, cellular components, and molecular functions—and Kyoto Encyclopedia of Genes and Genomes (KEGG) pathway analysis using R software [31–33]. Gene function and pathway terms were retrieved and visualized in R software.

2.1.4. GSEA analyses of significant related genes

We analyzed gene function with GSEA [34]. The gene expression data matrix of the control and DR groups was imported into OmicStudio tools at https://www.omicstudio.cn/tool and the permutation index set to 1000. We used the GS score and P-value to analyze the core pathway of significant genes and considered the top 9 pathways with a $P < 0.05$ as significant.

2.1.5. Construction of PPI interaction network

To investigate gene interactions, we imported the list of significant genes into the STRING database (https://string-db.org/) [35] and constructed a PPI network. We exported interaction pairs with a score greater than 0.4 and visualized them using Cytoscape (version 3.9.1) [36]. Significant modules within the PPI network were identified using the MCODE [37] plugin, with parameters set to a degree cutoff of 2, a node score cutoff of 0.2, a K-score of 2, and a maximum depth of 100. To determine the most significant genes, we employed the CytoHubba [38] plugin within Cytoscape.

2.1.6. Significant interaction network analysis

GeneMANIA (http://www.genemania.org) is a web-based tool for generating gene function hypotheses, analyzing gene lists, and prioritizing genes for functional assays [39]. We utilized GeneMANIA to analyze the core regulatory network groups identified by MCODE and the 11 sites associated with AGER. We constructed their interaction network and conducted functional enrichment pathway screening.

2.1.7. Immune infiltration by MCPcounter analysis

We analyzed normalized data using MCP-counter [40] to obtain an immune cell infiltration matrix, examining 8 immune cell types and 2 stromal cell types. Dimensionality reduction was performed with the R package umap (version 0.2.7.0), and Z-scores were applied to the expression profiles. Data visualization was achieved using box plots created with the R package ggplot2. Additionally, a correlation heatmap was generated in R to evaluate the associations among immune cells within each population.

2.2. Validation

To further investigate whether ADIPOQ plays a significant role in the onset and progression of DR through the encoding of adiponectin and its involvement in the AGEs-RAGE axis, we independently validated the findings from the public database analysis.

2.2.1. Detection of the changes of key genes under different disease courses by scRNA-seq

2.2.1.1. DR rats models construction. Single cells were isolated from retinal specimens of five donor SD rats, comprising two from the control group at 0 weeks and one each from the experimental group at 2 weeks, 4 weeks, and 8 weeks of DR. The SD rats were acclimated to a standard diet for 1 week. Diabetes was induced in the experimental rats using streptozotocin (STZ) after an overnight fast, with STZ dissolved in citrate buffer. Two control rats received citrate phosphate buffer, while the remaining rats were administered STZ. Diabetes induction was confirmed by measuring fasting blood glucose concentrations on the third day post-STZ administration. Rats with blood glucose levels exceeding 200 mg/dL were selected for the experiment.

2.2.1.2. Tissue processing and cell purification. Diabetic animals were maintained on a high-sugar diet, and tail vein blood samples were regularly collected and measured to monitor glucose levels. Rats in both the experimental groups (2 weeks, 4 weeks, and 8 weeks) and the control group were anesthetized via intraperitoneal injection and positioned supine. The eyeballs were removed, and the corneoscleral limbus was cut. The eyes were then incised radially, and the anterior segment and vitreous were extracted. The iris was separated from the intact retina and placed in a protective solution. The tissues were transported on ice in DPBS and minced after the removal of the storage solution. The tissues were digested with PBS-FBS containing trypsin and DNase I, and dissociation was carried out at 37 °C for 40 min. Dissociated cells were collected every 20 min and filtered through a nylon cell strainer. Red blood cells were removed using a lysis solution, and the remaining cells were washed with DPBS-FBS. Cell viability was assessed using Trypan Blue staining and a cell counter.

2.2.1.3. 10x library preparation and sequencing. Beads, loaded with unique molecular identifiers (UMIs) and cell barcodes, were prepared to near-saturation to ensure each cell was paired with a bead in gel beads-in-emulsion (GEM) droplets. Following exposure to cell lysis buffer, polyadenylated RNA molecules hybridized to the beads. The beads were then collected into a single tube for reverse transcription. During cDNA synthesis, each cDNA molecule was tagged with the UMI and cell barcode at the 5' end. Briefly, 10 × beads underwent second-strand cDNA synthesis, adaptor ligation, and universal amplification. Sequencing libraries were prepared by enriching the 3' ends of transcripts associated with UMIs and cell barcodes through randomly interrupted whole-transcriptome amplification products. All subsequent procedures, including library construction, adhered to the standard manufacturer's protocol (CG000206 Rev. D). Sequencing libraries were quantified using a High Sensitivity DNA Chip (Agilent) on a Bioanalyzer 2100 and a Qubit High Sensitivity DNA Assay (Thermo Fisher Scientific). Libraries were sequenced on a NovaSeq6000 instrument (Illumina) in 2 x 150 bp mode. Further details are provided in the supplementary materials. The raw sequencing data have been deposited in the GEO database under accession number GSE209872.

2.2.1.4. Data analysis. We extracted the expression data of key genes relevant to diabetic retinopathy in mice, including ADIPOR1, ADIPOR2, PAQR4, PAQR6, PAQR7, ADIPOQ, COL20a1, and VEGFA. Genes not listed either could not be extracted from the available data or were not included due to their insufficient significance.

2.2.2. Detection of AGER related proteins

2.2.2.1. Patient inclusion. The study cohort included 11 control subjects and 31 patients with type 2 diabetes mellitus (T2DM), recruited from the Department of Ophthalmology at Zhujiang Hospital, Guangzhou, China. Mydriatic retinal fundus photography (Kowa FX-500S; Kowa, Tokyo, Japan) was used to document retinal conditions. DR severity was classified according to the American Academy of Ophthalmology protocol, defining PDR as the presence of neovascularization or hemorrhage in the retina or optic nerve [41]. A masked medical retina specialist graded the images on two separate occasions to ensure internal validity, achieving excellent agreement between the two assessments. The study protocol was approved by the Ethics Committee of Zhujiang Hospital, Southern Medical University. Written, informed consent was obtained from all participants. The inclusion criteria for patients refer to Supplementary Material S_2.

2.2.2.2. AGER related protein detection. ELISA detection was conducted to quantify the protein expression levels of soluble receptors for sRAGE, esRAGE, ADIPOQ, AGEs, and vascular endothelial growth factor (VEGF) in peripheral blood, using a commercially available kit (Jiang Lai, Shanghai, China) following the manufacturer's instructions. In brief, microplate wells pre-coated with

antibodies specific to AGEs (including sRAGE, esRAGE, ADIPOQ, and VEGF) were used. Standards and samples were pipetted into the wells, and after removing unbound substances and washing, horseradish peroxidase (HRP) was added. After another wash, a substrate solution was added to induce color development in proportion to the amount of AGEs present. The intensity of the resulting color was then measured.

3. Results

3.1. Bioinformatics mining

3.1.1. GSEA analysis for significant related genes of DR

The distribution of pathway gene sets across all gene expression data from DR patients and control samples was analyzed using GSEA software. The analysis parameters were set with a minimum gene set size of 5, a maximum gene set size of 5000, 1000 resampling iterations, and thresholds for statistical significance of a P-value <0.05 and a False Discovery Rate (FDR) < 0.25. GSEA revealed significant pathways associated with DR, including ocular pigment metabolism pathways such as retinol metabolism; protein and amino acid metabolism pathways such as arginine and proline metabolism, tyrosine metabolism, and phenylalanine metabolism; diabetes-related pathways such as oxidative phosphorylation, proximal tubule bicarbonate reclamation, and type I diabetes mellitus; and immune-related pathways such as allograft rejection and graft-versus-host disease (Fig. 1).

3.1.2. Differential analysis screening DEGs

A total of 19,171 DEGs were identified, comprising 14,732 up-regulated and 4,439 down-regulated genes, with an adjusted P-value <0.05 and a LogFC >1.1 between DR patients and control samples. The volcano plot for DEGs comparing DR and control samples is shown in Fig. 1A. The heatmap of the top 50 DEGs is presented in Fig. 1B. The boxplot illustrating the sample selection and grouping methods is shown in Fig. 2C.

3.1.3. GO term and KEGG pathway enrichment analysis of DEGs :

GO term and Kyoto Encyclopedia of Genes and Genomes (KEGG) pathway enrichment analyses were performed on up-regulated and down-regulated genes, with a minimum gene set size of 5, a maximum gene set size of 5000, a P-value <0.05, and a FDR

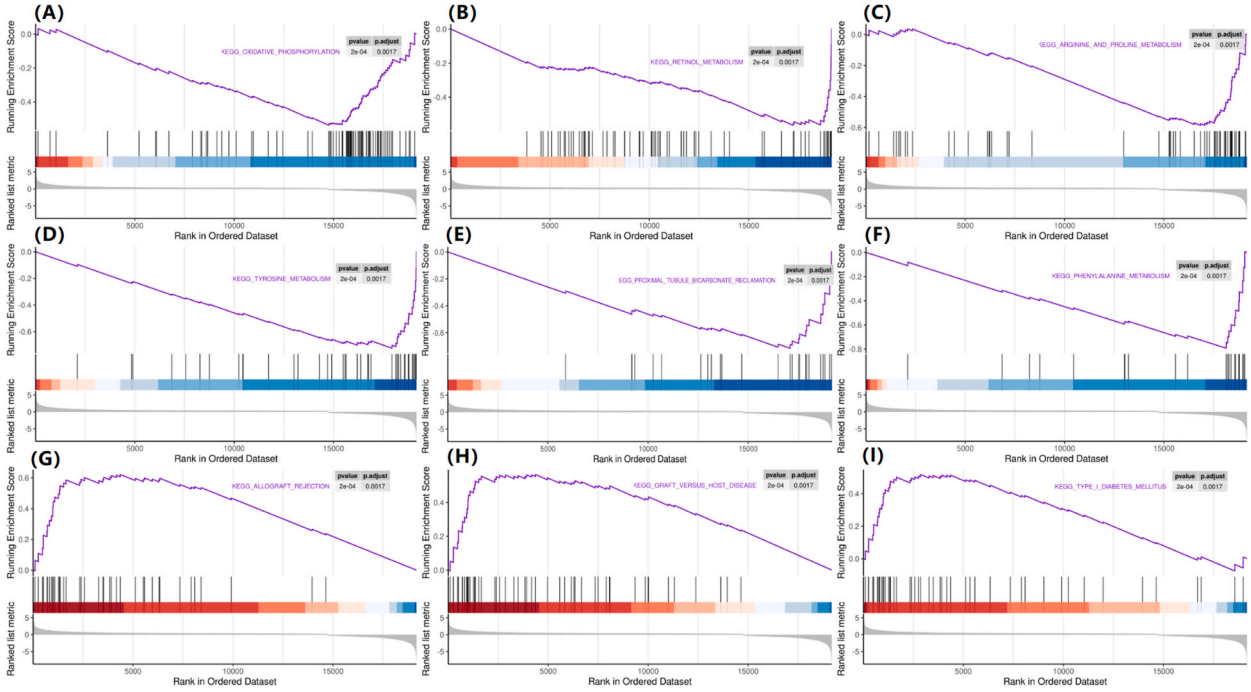

Fig. 1. Gene set enrichment analysis:
(A) Enrichment plot of 'OXIDATIVE_PHOSPHORYLATION' with enrichment score −0.52, FDR q-value 0.0016. (B) Enrichment plot of 'RETINOL_METABOLISM' with enrichment score −0.59, FDR q-value 0.0016. (C) Enrichment plot of 'ARGININE_AND_PROLINE_METABOLISM' with enrichment score −0.56, FDR q-value 0.0016. (D) Enrichment plot of 'TYROSINE_METABOLISM' with enrichment score −0.73, FDR q-value 0.0016. (E) Enrichment plot of 'PROXIMAL_TUBULE_BICARBONATE_RECLAMATION' with enrichment score −0.77, FDR q-value 0.0016. (F) Enrichment plot of 'PHENYLALANINE_METABOLISM' with enrichment score −0.77, FDR q-value 0.0016. (G) Enrichment plot of 'ALLOGRAFT_REJECTION' with enrichment score 0.67, FDR q-value 0.0016. (H) Enrichment plot of 'GRAFT_VERSUS_HOST_DISEASE' with enrichment score 0.61, FDR q-value 0.0016. (I) Enrichment plot of 'TYPE_I_DIABETES_MELLITUS' with enrichment score 0.66, FDR q-value 0.0016.

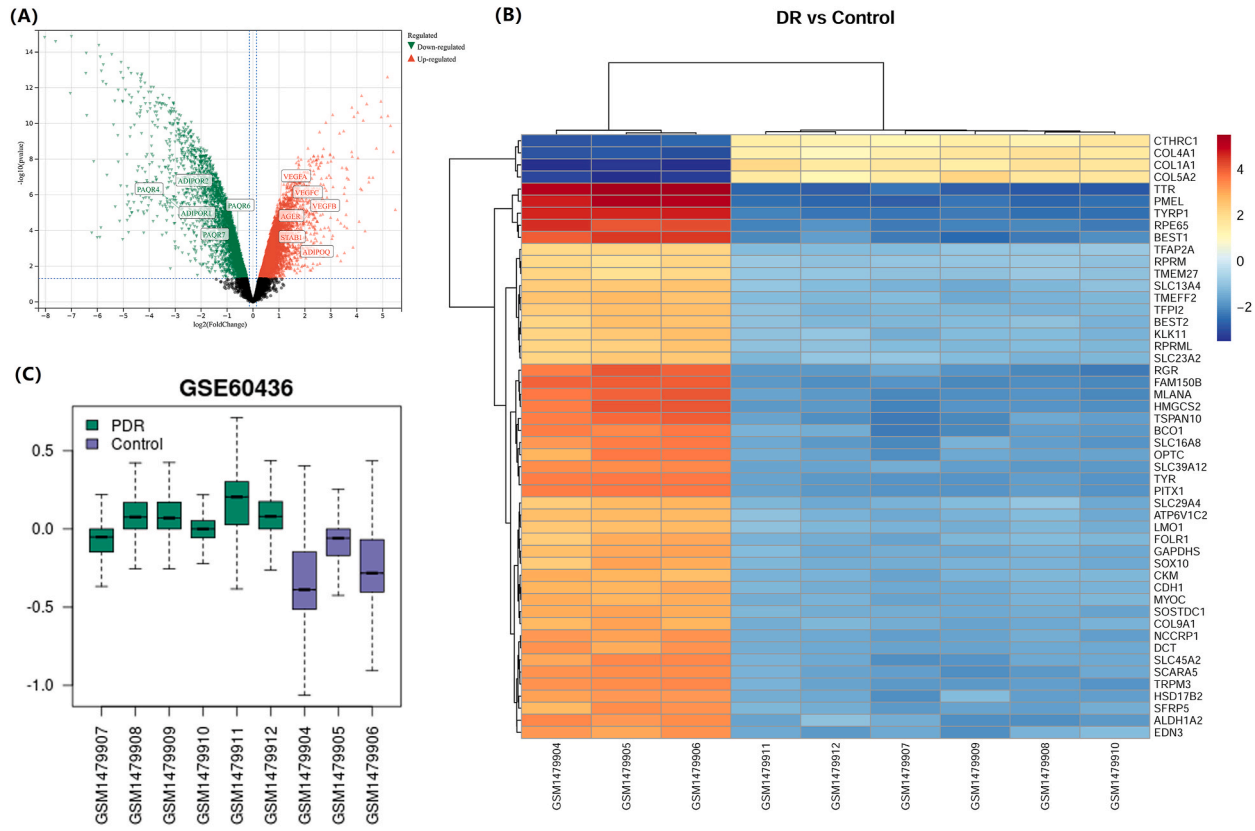

Fig. 2. **(A)** Volcano map shows expression levels of DEGs.
(B) Heatmap of the top-50 DEGs. **(C)** Box map of selected samples and samples grouping.

<0.25 considered statistically significant. The results of the GO analysis for Biological Process (BP), Cellular Component (CC), and Molecular Function (MF) terms for significant genes associated with DR are illustrated in Fig. 3 (A, B, and C). The KEGG pathway enrichment results for these significant genes are depicted in Fig. 3D. Significant genes were predominantly enriched in the following GO-BP terms: sensory perception of light stimulus, developmental pigmentation, secondary metabolite biosynthetic process, vitamin A metabolic process, pigment metabolic process, and pigment biosynthetic process. For GO-CC terms, enrichment was observed in the collagen-containing extracellular matrix, the collagen trimer, the complex of collagen trimers, and the fibrillar collagen trimer. In terms of GO-MF, significant enrichment was found in extracellular matrix structural constituents and platelet-derived growth factor binding. KEGG pathway enrichment highlighted significant associations with protein digestion and absorption, the AGEs-RAGE signaling pathway in diabetic complications, ECM-receptor interaction, focal adhesion, tyrosine metabolism, retinol metabolism, and relaxin signaling pathway. The GO and KEGG enrichment results are highly consistent with the GSEA findings, providing a comprehensive understanding of the potential pathogenesis of DR.

3.1.4. Analyzing significant related genes in DR using a PPI network

To further elucidate the regulatory and interaction relationship, the significant related genes were imported into the STRING database and visualized in Cytoscape (version 3.8.2). The STRING database identified a PPI-network of 205 protein products and 603 edges (interaction relationships). We used the network analysis tool of Cytoscape to calculate the interaction degree between each site and divided the interaction network into four sub circled networks (Fig. 4A). Then we extracted 11 hub genes-ADIPOQ, VEGFA, PAQR6, PAQR7, STAB1, ADIPOR2, ADIPOR1, PAQR4, AGER, VEGFB, VEGFC- from the interaction network, which are significantly related to ADIPOQ(Fig. 4B). We used the MCODE plug-in in Cytoscape to determine four significant interacted modules from the interaction network (Fig. 4C and Table 2). Through the interaction network and sub-networks, we established that ADIPOQ, AGER, and the collagen family may play an important role in the development of DR. The top ten hub sites obtained by five algorithms, MCC, DMNC, MNC, Degree, and EPC, in the cytohubba plug-in, are shown in Table 3. The overlap of hub genes among the five algorithms was verified by a Venn diagram (Fig. 4D and Table 3).

3.1.5. Construction and analysis of significant PPI sub-networks

The GeneMANIA is used to predict functionally similar sites of hub genes. We analyzed the 10 sites of the collagen family screened by MCODE and 11 sites significantly related to AGER, and obtained two key site interaction networks, The hub genes were located in

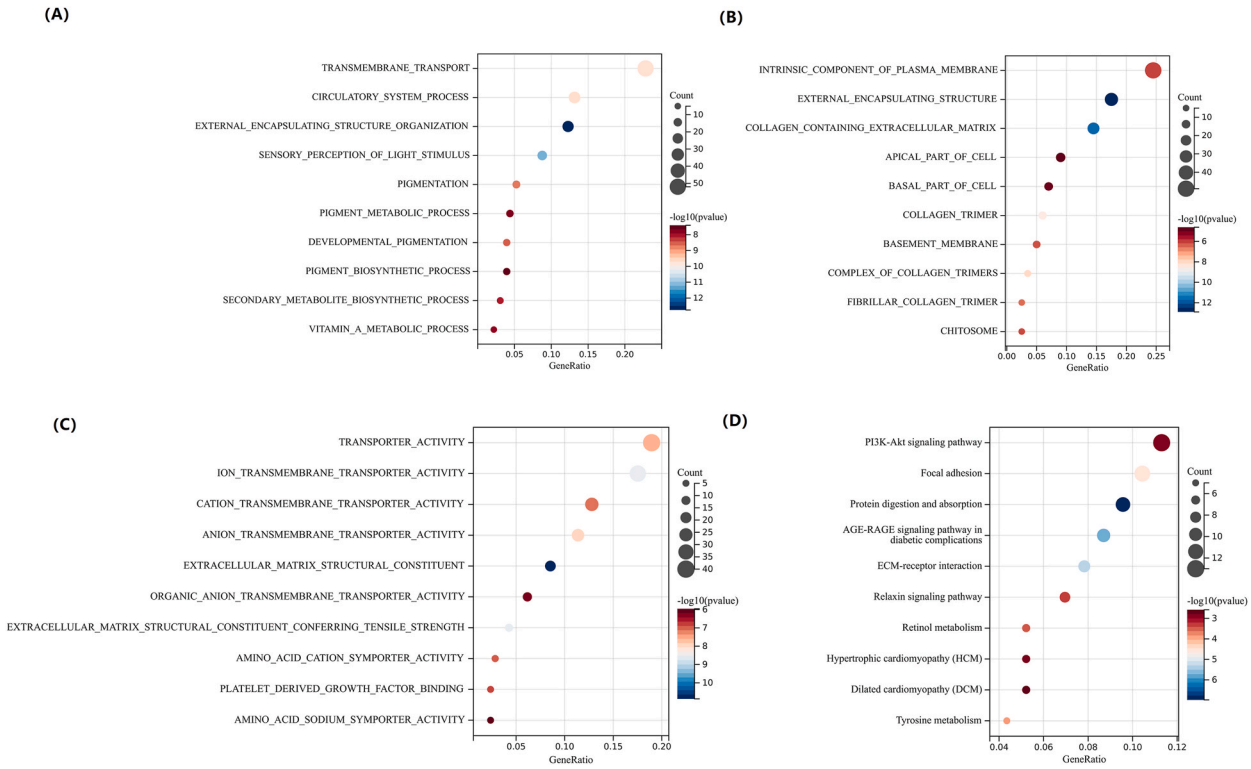

Fig. 3. GO-KEGG analysis for significant related genes:
(A) GO enrichment analysis on the Biological Process (BP) terms of the significant related genes. **(B)** GO enrichment analysis on the Cellular Component (CC) terms of the significant related genes. **(C)** GO enrichment analysis on the Molecular Function (MF) terms of the significant related genes. **(D)** KEGG terms in the enrichment analysis of the significant related genes.

the inner circle, while the predicted genes were in the outer circle (Fig. 5). The functions of 11 sites significantly related to AGER mainly focused on growth factor related pathways and angiogenesis, while the functions of the collagen family mainly focused on extracellular matrix structural constituents, collagen trimer, and collagen-containing extracellular matrix. The results of enrichment pathways and functions of the AGER related sites and collagen family are consistent with the results of GO-KEGG analysis, reflecting the significant role of the AGER related sites and collagen family in DR.

3.1.6. Immune infiltration between DR and control samples

Uniform Manifold Approximation and Projection (UMAP) was performed on two groups. Blue points indicate DR samples, and red points indicate normal control samples, which showed that there was a significant difference ($P < 0.05$) in immune cell infiltration between the DR and control samples (Fig. 6A). The cor-heatmap (Fig. 6B) result showed that NK cells and CD8+T cells (value = 0.939), myeloid dendritic cells and CD8+T cells (value = 0.913) had a positive correlation with each other. Neutrophils had a significant negative correlation with the monocytic lineage (value = − 0.845). Compared with normal control samples from healthy donors, the box plot of the immune cells showed that, T cells, $CD8^+$ T cells, cytotoxic lymphocytes, B lineage, NK cells, monocytic lineage, myeloid dendritic cells, endothelial cells, and fibroblasts infiltrated statistically more, while neutrophils infiltrated statistically less in DR samples (Fig. 6C).

3.2. Validation

3.2.1. Detection of the changes of key molecules under different disease course by scRNA-seq

3.2.1.1. Baseline characteristics of research subjects. The single-cell sequencing data has been submitted to the GEO database under the accession number GSE209872. This dataset contains sequencing data from the retinal microglia of four rats: two at 0 weeks old, one at 2 weeks, one at 4 weeks, and one at 8 weeks old. To validate our findings, we analyzed the gene expression profiles of these tissues.

3.2.1.2. scRNA-seq result. High expression of Adipor1 was observed throughout the progression of DR, whereas Adipor2 expression decreased to undetectable levels as the disease advanced. PAQR4 and PAQR7 were consistently highly expressed throughout the disease course, while PAQR6 was rarely expressed. Adipoq expression diminished over the course of the disease. Additionally, Col20a1

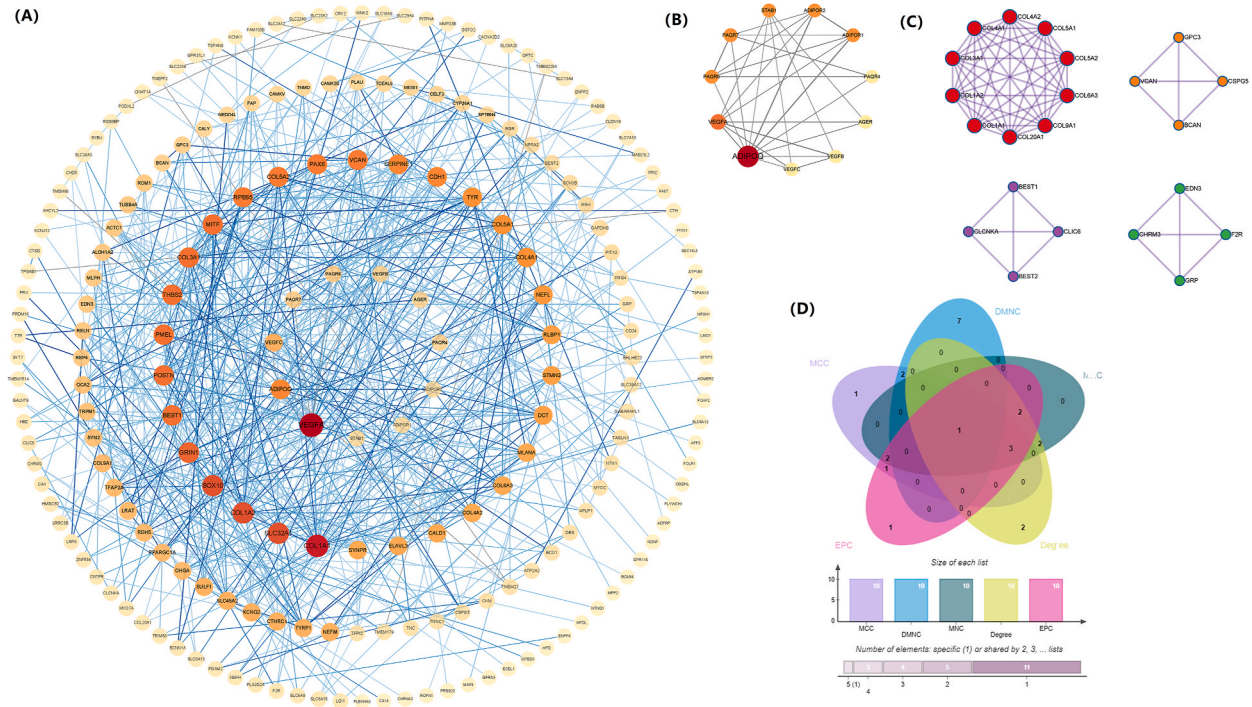

Fig. 4. (A) Top-250 sites filtered into the PPI network that contained 205 nodes and 603 edges in DR. (B) Sub-network for 11 sites significantly related to AGER. (C) Sub-networks for MCODE sub-networks. (D) Venn map for hub genes five algorithms.

and Vegfa were notably expressed at the onset of DR (Fig. 7, Table 4).

3.2.2. *Detection of the expression of AGER related sites*

3.2.2.1. Baseline characteristics of study subjects. In the validation phase, 42 participants were recruited and categorized into four groups based on the stage of DR: Proliferative DR (PDR, n = 11), Non-Proliferative DR (NPDR, n = 10), Diabetes Mellitus (DM, n = 10), and a Control group (n = 11). The groups were matched for age and sex. Basic information, clinical test results, and laboratory data for all participants are presented in Table 1.

3.2.2.2. ELISA to explore AGEs-RAGE pathway molecules. The levels of soluble receptor for sRAGE, esRAGE, ADIPOQ, vascular endothelial growth factor (VEGF), and AGEs in the peripheral blood of 42 volunteers were measured by ELISA. The results showed that the levels of sRAGE, esRAGE, and ADIPOQ decreased progressively from the Control group to DM, NPDR, and PDR groups. Conversely, the levels of VEGF and AGEs increased in the same sequence from Control to DM, NPDR, and PDR groups (Fig. 8, Table 5).

4. Discussion

Diabetic retinopathy is a microangiopathy affecting the retina, characterized by alterations in the vascular wall and changes in blood rheological properties. Typical histopathological changes include the loss of pericytes and endothelial cells, as well as thickening of the basement membrane [2].

4.1. *DR-ADIPOQ-AGEs-RAGE: a vicious positive feedback loop*

In the ELISA results, the level of adiponectin in the peripheral blood of patients with PDR was significantly lower compared to the control group. Similarly, ADIPOQ levels were reduced in our single-cell sequencing analysis. Adiponectin, a protein predominantly secreted by adipocytes, is encoded by the ADIPOQ gene and is known to decrease in diabetic patients. This protein plays a crucial role in protecting against insulin resistance and excessive hepatic lipid accumulation, and exhibits anti-inflammatory effects [42–44]. Previous studies have reported a decline in adiponectin levels in diabetic retinopathy [45]. Collectively, these findings indicate a downward trend in adiponectin concentrations associated with diabetic retinopathy.

The interaction between AGEs and receptor for RAGEs is crucial to the pathogenesis of DR and its associated complications [3]. Dysregulation of the AGEs-RAGE axis significantly contributes to DR development. Specifically, AGEs-RAGE interactions activate signaling proteins and transcription factors, which lead to altered cellular responses. This activation promotes the NADPH oxidase

Table 1
Basic information, clinical test results and laboratory data of all participants.

Characteristics	PDR (n = 11)	NPDR(n = 10)	DM(n = 10)	CON(n = 11)	P-value
Age (year)	56.73 ± 7.39	55.50 ± 6.54	64.70 ± 5.93	53.55 ± 10.21	0.028
BMI ($kg{\cdot}m^2$)	24.23 ± 3.87	23.07 ± 3.07	24.89 ± 5.01	21.24 ± 2.92	0.135
SBP(mmHg)	141.00 ± 24.01	130.30 ± 24.45	148.60 ± 11.10	128.09 ± 19.61	0.052
DBP(mmHg)	80.91 ± 15.55	72.60 ± 10.46	87.00 ± 9.50	78.82 ± 5.88	0.016
Duration of diabetes (year)	6.27 ± 5.46	8.80 ± 5.16	4.70 ± 4.24	0.00 ± 0.00	<0.001
Gender					0.042
Female	7 (63.64 %)	5 (50.00 %)	4 (40.00 %)	8 (72.73 %)	
Male	4 (36.36 %)	5 (50.00 %)	6 (60.00 %)	3 (27.27 %)	
Alcohol					0.449
Yes	0 (0.00 %)	0 (0.00 %)	0 (0.00 %)	0 (0.00 %)	
No	11 (100.00 %)	10 (100.00 %)	10 (100.00 %)	11 (100.00 %)	
Smoking					0.749
Yes	1 (9.09 %)	1 (11.11 %)	1 (10.00 %)	0 (0.00 %)	
No	10 (90.91 %)	8 (88.89 %)	9 (90.00 %)	11 (100.00 %)	
Hypertension					0.008
Yes	10 (90.91 %)	4 (44.44 %)	5 (50.00 %)	2 (18.18 %)	
No	1 (9.09 %)	5 (55.56 %)	5 (50.00 %)	9 (81.82 %)	
HbA1c(%)	6.50 ± 0.82	8.13 ± 2.76	7.48 ± 1.75	5.45 ± 0.38	<0.001
TG(mmol/l)	2.04 ± 1.30	2.04 ± 1.44	1.79 ± 0.88	1.79 ± 0.94	0.945
TC(mmol/l)	4.76 ± 1.18	5.35 ± 2.07	4.66 ± 1.29	4.77 ± 1.54	0.705
HDL(mmol/l)	1.32 ± 0.43	1.31 ± 0.66	1.14 ± 0.32	1.14 ± 0.15	0.764
LDL(mmol/l)	2.71 ± 1.02	3.74 ± 1.47	2.94 ± 1.22	3.36 ± 1.13	0.141
FPG(mmol/L)	6.19 ± 1.36	7.81 ± 4.20	7.14 ± 2.91	5.03 ± 0.52	0.071
ALT(U/L)	27.91 ± 24.18	18.20 ± 4.92	26.30 ± 15.54	15.27 ± 7.64	0.211
AST(U/L)	20.27 ± 8.47	17.50 ± 4.03	26.20 ± 17.73	15.00 ± 3.97	0.231
TBIL(mmol/L)	5.25 ± 1.81	5.65 ± 3.25	10.06 ± 6.14	8.08 ± 3.55	0.057
DBIL(mmol/L)	3.20 ± 2.46	2.24 ± 0.89	4.21 ± 2.27	3.39 ± 1.24	0.061
TBA(mmol/L)	2.48 ± 1.70	3.77 ± 2.86	13.22 ± 12.71	8.21 ± 7.94	0.037
Creatinine (μmol/l)	169.18 ± 91.53	165.70 ± 118.53	82.78 ± 27.81	65.73 ± 15.21	0.002
magnesium (mmol/L)	0.93 ± 0.14	0.85 ± 0.09	0.83 ± 0.08	0.90 ± 0.09	0.355

Values are presented as mean ± standard deviation or number (%).
*P < 0.05. *p* values were compared by Kruskal-Wallis test or $\chi 2$ test as appropriate.
BMI, body mass index; SBP, systolic blood pressure; DBP, diastolic blood pressure.
TG, triglycerides; TC, cholesterol; HDL, high-density lipoprotein cholesterol.
LDL, low-density lipoprotein cholesterol; FPG, fasting plasma glucose; ALT, alanine aminotransferase.
AST, aspartate transaminase; TBIL, total bilirubin; DBIL, direct bilirubin; TBA, Total Bile Acid.

Table 2
MCODE protein networks and enrichment analysis.

Color	MCODE	GO	Description	Log10(P)
red	MCODE_1	M3005	NABA COLLAGENS	−28.8
red	MCODE_1	R-HSA-8948216	Collagen chain trimerization	−28.8
red	MCODE_1	R-HSA-1650814	Collagen biosynthesis and modifying enzymes	−26.8
green	MCODE_2	R-HSA-416476	G alpha (q) signalling events	−8.6
green	MCODE_2	R-HSA-373076	Class A/1 (Rhodopsin-like receptors)	−7.8
green	MCODE_2	hsa04080	Neuroactive ligand-receptor interaction	−7.7
purple	MCODE_3	GO:0006821	chloride transport	−9.9
purple	MCODE_3	GO:0015698	inorganic anion transport	−9
purple	MCODE_3	GO:0006820	anion transport	−7.3
orange	MCODE_4	R-HSA-4420332	Defective B3GALT6 causes EDSP2 and SEMDJL1	−12.9
orange	MCODE_4	R-HSA-3560801	Defective B3GAT3 causes JDSSDHD	−12.9
orange	MCODE_4	R-HSA-3560783	Defective B4GALT7 causes EDS, progeroid type	−12.9

Log10(P) represents the level of statistical significance. This value indicates the degree to which genes associated with a particular function or pathway are enriched in your gene collection, and whether this enrichment is significant.

system, resulting in the formation of reactive oxygen species (ROS) and subsequent cellular oxidative damage [16]. These processes can also induce changes in microcirculation [17].

It is promising that adiponectin has been reported to provide significant protection against AGEs-induced endothelial dysfunction and effectively counteract the dysregulation of the AGEs-RAGE axis [28]. Adiponectin exerts its protective effects primarily through downstream receptor signaling. This involves various receptors, including the PAQR family (which encompasses progestin and ADIPOQ receptors) and the ADIPOR family (adiponectin receptors). ADIPOQ acts as an intermediary linking adiponectin to the AGEs-RAGE axis. Adiponectin transmits binding signals through PAQR and ADIPOR receptors via the AMP-activated protein kinase (AMPK) and p38 MAPK kinase pathways, thereby protecting against AGEs and lipid overload by accelerating fatty acid oxidation and

Table 3
Five operation modes of Cytohubba and Top-10-Genes selection.

MCC	DMNC	MNC	Degree	EPC
COL1A1	STAB1	VEGFA	VEGFA	COL1A1
COL1A2	CTHRC1	COL1A1	COL1A1	VEGFA
COL3A1	COL4A2	COL1A2	SOX10	COL1A2
COL5A2	TRPM1	SOX10	SLC32A1	THBS2
COL4A1	MLANA	THBS2	COL1A2	POSTN
VEGFA	COL6A3	POSTN	GRIN1	COL3A1
POSTN	MLPH	GRIN1	THBS2	SOX10
COL6A3	SULF1	COL3A1	POSTN	COL5A2
COL5A1	TYRP1	COL5A2	PMEL	COL5A1
COL4A2	VEGFA	SLC32A1	MITF	VCAN

MCC: Maximum group centrality, DMNC: Maximum neighborhood component density, MNC: Maximum neighborhood component, EPC: Edge penetration component.

other metabolic effects [46–48].

However, adiponectin levels are often reduced in patients with DR, diminishing its inhibitory effect on the AGEs-RAGE axis. This reduction may enhance the pathogenic effects of the AGEs-RAGE axis, leading to an increased incidence of DR. Consequently, a vicious positive feedback loop is established, wherein decreased adiponectin exacerbates AGEs-RAGE-induced DR pathogenesis. This suggests that adiponectin could play a crucial role in regulating DR through its interaction with the AGEs-RAGE axis.

4.2. Potential pathogenic mechanisms of DR indicated by key molecules

Adiponectin interacts with two specific cell surface receptor subtypes, AdipoR1 and AdipoR2 [48], both of which are highly expressed in the retina [49]. AdipoR1 is primarily linked to the activation of the AMPK pathway, which inhibits hepatic glycogenesis and promotes increased fatty acid oxidation. In contrast, AdipoR2 activates the peroxisome proliferator-activated receptor alpha (PPARα) nuclear receptor pathway, initiating fatty acid oxidation while reducing tissue inflammation and oxidative stress [50]. In our study, AdipoR1 expression was consistently observed throughout the disease progression, whereas AdipoR2 expression remained low. This reduced expression of AdipoR2 may exacerbate oxidative stress and inflammatory responses in the retina, potentially contributing to the development of diabetic retinopathy through oxidative stress as a primary mechanism.

PAQR4, PAQR6 and PAQR7 all belong to the PAQR family of transmembrane proteins, along with the lipocalin receptor and the membrane progesterone receptor [51]. PAQR4's function is unknown, but it may be related to the insulin signalling pathway because of its ability to interact with insulin receptor substrate 1 (IRS1) and phosphatidylinositol kinase (PI3K) [52]. PAQR6 and PAQR7 are membrane progesterone receptors that bind progesterone and other steroid hormones and regulate cell proliferation, differentiation, and apoptosis [53]. PAQR7 is also able to regulate neuronal growth and synapse formation [54]. Our observation of high expression of PAQR4 and PAQR7 and low expression of PAQR6 may indicate that: the insulin signalling pathway of the cell is activated, promoting cell metabolism and growth. The progesterone signalling pathway of the cell is activated, promoting cell differentiation and survival. The PAQR6 signalling pathway of the cell is inhibited, reducing cell proliferation and apoptosis.

Another notable finding is the significant interaction of several collagen family members in the PPI network, including COL1, COL3, COL4, COL5, COL6, COL9, and COL20. Collagen, a major component of the extracellular matrix, plays a crucial role in the formation of membrane structures, extracellular matrix maintenance, and the preservation of microcirculatory structure [55]. The prominent expression of collagen family members in DR highlights increased matrix and basement membrane connective tissue deposition, which may be implicated in the pathogenesis of proliferative retinopathy in diabetic patients. Notably, single-cell sequencing revealed high expression of COL20, which may contribute to vascular fibrosis and vascular calcification in individuals with retinopathy.

4.3. Molecular changes in ELISA and multiple possibilities for DR pathogenesis

In our ELISA experiments, we observed elevated levels of AGEs as the disease progressed. The primary pathway for AGE formation is the polyol pathway, which becomes activated under chronic hyperglycemic conditions, leading to increased AGE synthesis and subsequent biochemical damage in retinal tissue. This mechanism involves both receptor for RAGE-dependent and -independent pathways [56]. Some studies have assessed AGE levels in vivo using skin autofluorescence and reported that AGE levels are significantly higher in diabetic patients compared to non-diabetic individuals. They found that elevated AGE scores were independently associated with the progression of diabetic retinopathy [57]. Furthermore, AGEs can induce aberrant angiogenesis by binding to RAGE, activating the RhoA/ROCK signaling pathway, and promoting moesin phosphorylation [58]. Our bioinformatics analyses also highlighted the AGEs-RAGE pathway as crucial for the development of diabetic retinopathy.

However, there are additional pathways contributing to DR that are not mediated through RAGE receptors. For instance, the loss of peripapillary retinal cells, a common microvascular complication of diabetes, is not mitigated by the absence of Ager. Instead, it persists in both type 1 and type 2 diabetic mouse models; the absence of Ager affects retinal permeability, cellular capillarity, microglia activation, and gliomagenesis of ocular Müller cells [59]. Therefore, further in-depth studies are necessary to elucidate the complex underlying mechanisms of diabetic retinopathy.

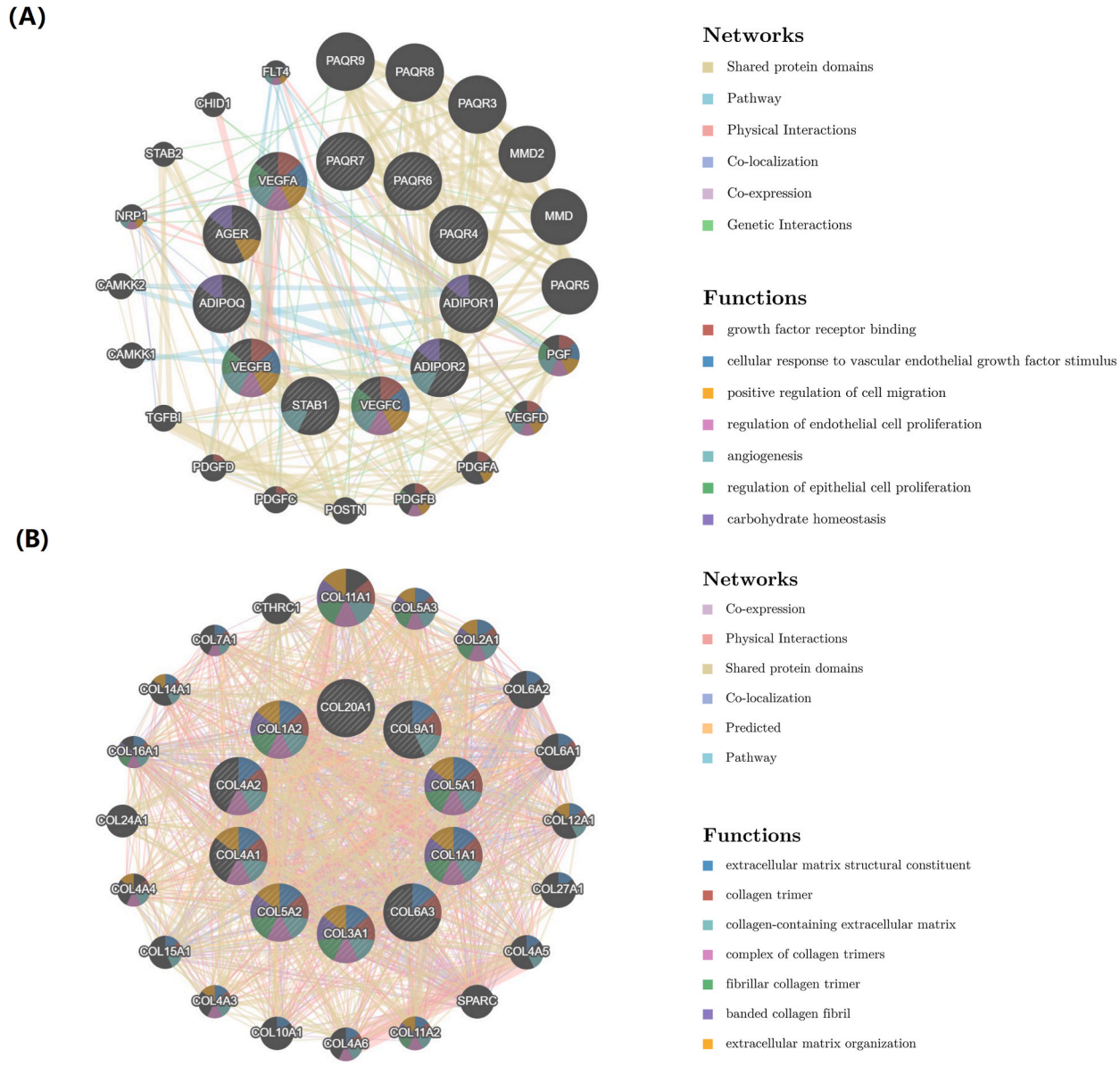

Fig. 5. (A) Functionally similar sites interaction network for 11 sites significantly related to AGER. (B) Functionally similar sites interaction network for Collagen family.

In addition, VEGF is expressed in the course of DR and VEGF action contributes to angiogenesis in DR [60,61]. Certain metabolically driven hypoxia-inducible factor 1 (HIF-1) non-dependent pathways can also regulate the expression of VEGF-A [62]. VEGF-A contributes to vascular proliferation and can restore the supply of oxygen and energy substrates to the retina. This is consistent with our assay.

4.4. RAGE centred inflammation-associated immune infiltration

RAGE is expressed in retinal glial cells in the inner retina, thereby implicating RAGE as a major player in the recruitment of immune cells that induce inflammation as retinopathy progresses [63]. Our analyses showed that, in addition to Neutrophils, CD4+T cells, CD8+T cells, B cells, Myeloid dendritic cells and Macrophage were significantly infiltrated in the inflammatory tissues of DR patients. Studies have shown that the expression of RAGE encoding gene AGER is important for the homing of mature dendritic cells to lymph nodes, where they physically interact with T lymphocytes and activate T lymphocytes [64]. In addition, RAGE also seems to have the role of promoting macrophage cytotoxicity and enhancing cytotoxicity in immune cells, recent experiments proofed that in vitro, incubation of wild-type bone marrow derived macrophages into CML-AGE ligand increased M1 (CD86) expression and decreased M2

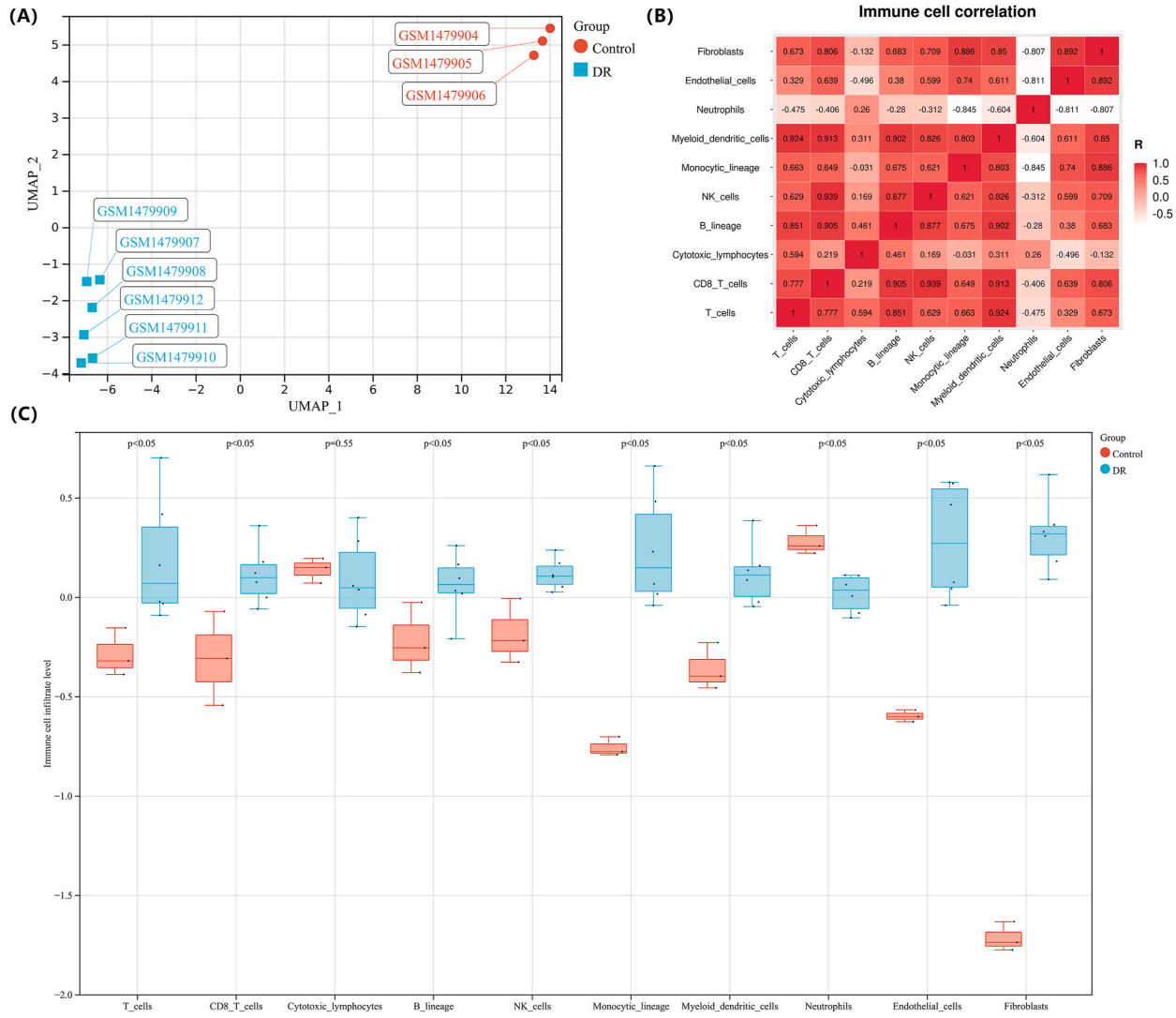

Fig. 6. (A) Umap plot for samples in GSE60436. (B) Correlation matrix of infiltration degree of immune cells in RA samples. (C) Box plot for immune cells infiltration degree.

(arginase 1) expression [65], The activation of RAGE in retina by local or circulating ligands such as AGEs and S100B leads to changes in the activities of various retinal cells including Müller glia, retinal microglia, RPE, and retinal endothelial cells [66]. What's interesting is that in our study, we observed that Fibroblasts and Endothelial cells were both seemed enhancing of infiltration in DR-patient samples, the activation of these immune cells and stromal cells provides new insights into the deep mechanism research and diagnostic scheme for DR.

Gene bioinformatics can provide a possible molecular targeting mechanism for the prevention and treatment of diabetic retinopathy. We combine immunoinfiltration analysis and GSEA analysis to dig out possible targeted gene data from multiple angles and at a deep level. At the same time, single-cell sequencing of rats was carried out, and the expression changes of adiponectin were verified by combining with the serum ELISA expression level of patients. Increased confidence in the results. However, we also have certain limitations. First, larger clinical sample sizes are needed to verify the expression of key genes. Secondly, more informatics analysis methods can be applied to explain this problem to enrich our horizons.

5. Conclusion

Adiponectin plays a central role in regulating DR through a positive feedback loop involving the ADIPOQ gene and the AGEs-RAGE axis. Additionally, the activation and enhancement of fibroblasts, endothelial cells, and microglia offer new immunological insights into the underlying mechanisms of DR and potential diagnostic approaches. Our study clarifies common modes of tissue damage in the microcirculation associated with DR and investigates various potential molecular mechanisms underlying its pathogenesis. These

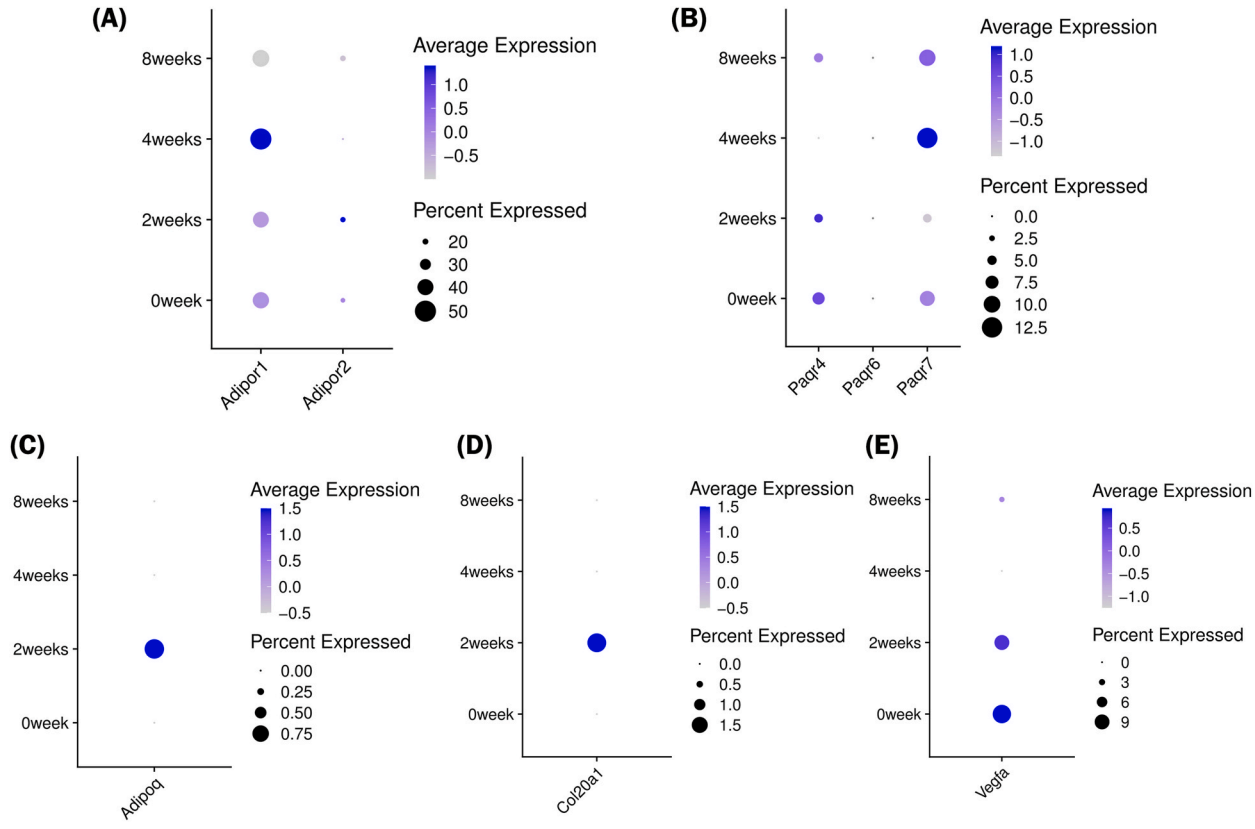

Fig. 7. DotPlot of key genes detected by single-cell sequencing
(A) DotPlot of ADIPOR1 and ADIPOR2 in single-cell sequencing (B) DotPlot of PAQR4, PAQR6 and PAQR7 in single-cell sequencing (C) DotPlot of ADIPOQ in single-cell sequencing (D) DotPlot of COL20a1 in single-cell sequencing (E) DotPlot of VEGFA in single-cell sequencing.

findings hold significant clinical and societal value by potentially reducing the incidence of blindness and improving the quality of life for patients with DR.

Funding sources

Thanks to the fundings: President's Fund of Zhujiang Hospital of Southern Medical University [grant yzjj2023ms05]; Medical Scientific Research Foundation of Guangdong Province, China [grant A2023423].

Ethics approval and consent to participate

Our study was performed in accordance with the ethical standards established by the 1964 Declaration of Helsinki and its later amendments, the International Conference on Harmonisation, Good Clinical Practice guidelines and all applicable laws and regulations. The animal study was reviewed and approved by the Scienceand Technology Commission of Shanghai Municipality. And the research has been registered on Chinese clinical trial registry (ChiCTR1800016357).

Data availability statement

The GEO dataset can be found in GSE60436 in https://www.ncbi.nlm.nih.gov/geo/ Single-cell assay data can also be found in GSE209872 in https://www.ncbi.nlm.nih.gov/geo/ The other original data can be asked from the authors if needed. All analysis was conducted by R 4.2.3.

CRediT authorship contribution statement

Min Fu: Methodology, Data curation. **Li Zhengran:** Writing – original draft, Visualization, Software, Methodology, Formal analysis. **Li Yingli:** Writing – review & editing, Validation, Methodology. **Wu Tong:** Validation, Methodology. **Cai Liyang:** Investigation, Conceptualization. **Guo Xi:** Supervision, Resources. **Yang Xiongyi:** Software, Resources. **Cao Mingzhe:** Supervision, Project

Table 4
Expression of hub genes by single-cell sequencing.

feature.plot	Average expression	Percent expressed	id	Scaled expressed
Adipor1	0.9200933	40.50633	0week	−0.13588386
Adipor2	0.3225226	17.72152	0week	0.01154078
Adipor1	0.8809068	39.63964	2weeks	−0.25061947
Adipor2	0.3736477	18.91892	2weeks	1.40547054
Adipor1	1.4397831	50	4weeks	1.38573501
Adipor2	0.2998321	12.5	4weeks	−0.60711815
Adipor1	0.6252277	41.46341	8weeks	−0.99923168
Adipor2	0.2923949	19.5122	8weeks	−0.80989316
Vegfa	0.176368304	11.3924051	0week	0.9335066
Vegfa	0.155034286	9.009009	2weeks	0.669898
Vegfa	0	0	4weeks	−1.2457455
Vegfa	0.071873417	2.4390244	8weeks	−0.3576591
PAQR4	0.09948703	6.962025	0week	0.5758277
PAQR6	0	0	0week	Na
PAQR7	0.10868069	8.860759	0week	−0.2262901
PAQR4	0.11766198	4.504505	2weeks	0.9251285
PAQR6	0	0	2weeks	Na
PAQR7	0.07351819	4.504505	2weeks	−1.2122567
PAQR4	0	0	4weeks	−1.3361935
PAQR6	0	0	4weeks	Na
PAQR7	0.15921539	12.5	4weeks	1.190717
PAQR4	0.06095234	4.878049	8weeks	−0.1647627
PAQR6	0	0	8weeks	Na
PAQR7	0.12558922	9.756098	8weeks	0.2478298
Adipoq	0	0	0week	−0.5
Adipoq	0.01561895	0.9009009	2weeks	1.5
Adipoq	0	0	4weeks	−0.5
Adipoq	0	0	8weeks	−0.5
Col20a1	0	0	0week	−0.5
Col20a1	0.027680945	1.8018018	2weeks	1.5
Col20a1	0	0	4weeks	−0.5
Col20a1	0	0	8weeks	−0.5

Adipor: Adiponectin Receptor 1, Adipor2: Adiponectin Receptor 2, Vegfa: Vascular Endothelial Growth Factor A, Adipoq: Adiponectin, PAQR4: Progestin And AdipoQ Receptor Family Member 4, PAQR6: Progestin And AdipoQ Receptor Family Member 6, PAQR7: Progestin And AdipoQ Receptor Family Member 7, Col20a1: Collagen Type XX Alpha 1 Chain.

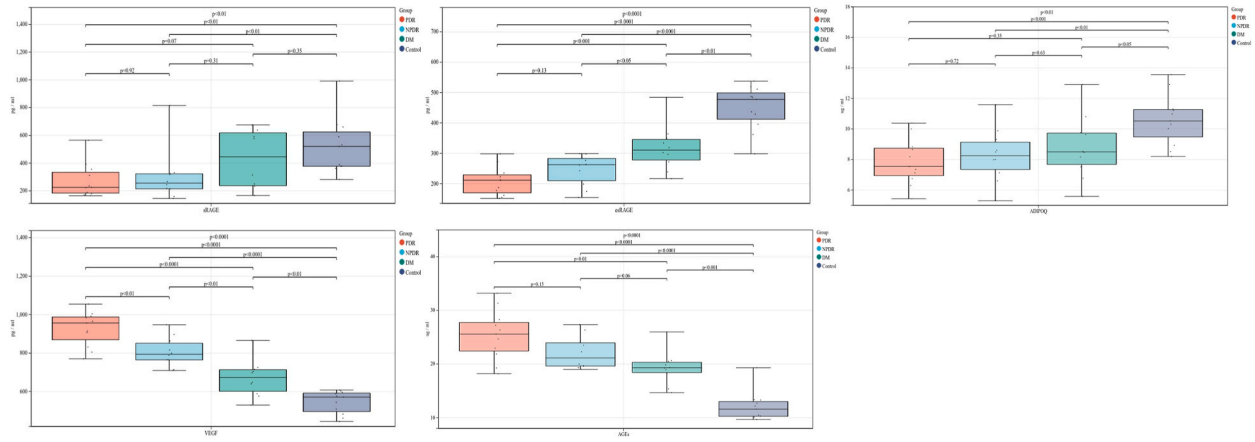

Fig. 8. The Box plot shows the ELISA detection results of 5 sites
DR: Diabetes retinopathy, PDR: Proliferative diabetes retinopathy, NPDR: non-proliferative diabetes retinopathy, ADIPOQ: Adiponectin, AGEs: Advanced glycation end products, sRAGE: The receptor of advanced glycation end products, esRAGE: Endogenous secreted receptor of advanced glycation end products, VEGF: Vascular endothelial growth factor.

Table 5
ELISA detection of patient serum.

Factor	Sample source	PDR	NPDR	DM	Control
sRAGE(pg/ml)	serum	274.233 ± 291.499	303.837 ± 158.55	426.336 ± 259.658	523.609 ± 250.372
esRAGE(pg/ml)	serum	207.585 ± 90.648	245.276 ± 90.91	317.541 ± 166.567	448.732 ± 150.285
VEGF(pg/ml)	serum	925.751 ± 155.406	806.345 ± 140.967	669.165 ± 197.117	543.989 ± 99.323
ADIPOQ(ug/ml)	serum	7.783 ± 2.512	8.292 ± 3.298	8.816 ± 4.091	10.593 ± 2.97
AGEs(ug/ml)	serum	25.349 ± 7.838	22.112 ± 5.237	19.297 ± 6.707	12.104 ± 7.183

sRAGE: the soluble Receptor of Advanced Glycation Endproducts, esRAGE: the endogenous secretory Receptor of Advanced Glycation Endproducts, VEGF: Vascular Endothelial Growth Factor, ADIPOQ: Adiponectin, AGEs: Advanced Glycation End products.

administration, Investigation. **Yi Guoguo:** Writing – review & editing, Supervision, Funding acquisition.

Declaration of competing interest

The authors declare that they have no known competing financial interests or personal relationships that could have appeared to influence the work reported in this paper.

Acknowledgments

Not applicable.

Appendix A. Supplementary data

Supplementary data to this article can be found online at https://doi.org/10.1016/j.heliyon.2024.e36111.

References

[1] IDF diabetes atlas [Internet]. Diabetesatlas.org. [cited 2024 Feb 2]. Available from: http://www.diabetesatlas.org/.
[2] A.N. Kollias, M.W. Ulbig, Diabetic retinopathy, Dtsch Arztebl Int [Internet] (2010), https://doi.org/10.3238/arztebl.2010.0075.
[3] P. Ahuja, A. Waris, S.S. Siddiqui, A. Mukherjee, Single nucleotide variants of receptor for advanced glycation end-products (AGER) gene: is it a new opening in the risk assessment of diabetic retinopathy?—a review, J Genet Eng Biotechnol [Internet] 20 (1) (2022) 17, https://doi.org/10.1186/s43141-022-00297-5.
[4] R. Mehta, G. Shaw, P. Masschelin, S. Felix, M. Otgonsuren, A. Baranova, et al., Polymorphisms in the receptor for advanced glycation end-products (RAGE) gene and circulating RAGE levels as a susceptibility factor for non-alcoholic steatohepatitis (NASH), PLoS One [Internet] 13 (6) (2018) e0199294, https://doi.org/10.1371/journal.pone.0199294.
[5] S. Ramprasad, V. Radha, R.A. Mathias, P.P. Majumder, M.R.S. Rao, M. Rema, Rage gene promoter polymorphisms and diabetic retinopathy in a clinic-based population from South India, Early Years Educat. 21 (3) (2007) 395–401, https://doi.org/10.1038/sj.eye.6702239 [Internet].
[6] O. Kucukhuseyin, H. Yilmaz-Aydogan, C.S. Isbir, T. Isbir, Is there any association between GLY82 ser polymorphism of rage gene and Turkish diabetic and non diabetic patients with coronary artery disease? Mol Biol Rep [Internet] 39 (4) (2012) 4423–4428, https://doi.org/10.1007/s11033-011-1230-3.
[7] P. Pradhan, N. Upadhyay, A. Tiwari, L. P Singh, Genetic and epigenetic modifications in the pathogenesis of diabetic retinopathy: a molecular link to regulate gene expression, New Front Ophthalmol [Internet] 2 (6) (2016), https://doi.org/10.15761/nfo.1000145.
[8] A. Julius, W. Hopper, A non-invasive, multi-target approach to treat diabetic retinopathy, Biomed Pharmacother [Internet] 109 (2019) 708–715, https://doi.org/10.1016/j.biopha.2018.10.185.
[9] A. Stitt, T.A. Gardiner, N.L. Anderson, P. Canning, N. Frizzell, N. Duffy, et al., The AGE inhibitor pyridoxamine inhibits development of retinopathy in experimental diabetes, Diabetes 51 (9) (2002) 2826–2832, https://doi.org/10.2337/diabetes.51.9.2826 [Internet].
[10] M. Mishra, R.A. Kowluru, Epigenetic modification of mitochondrial DNA in the development of diabetic retinopathy, Invest Ophthalmol Vis Sci [Internet] 56 (9) (2015) 5133, https://doi.org/10.1167/iovs.15-16937.
[11] M.J. Morgan, Z.-G. Liu, Crosstalk of reactive oxygen species and NF-κB signaling, Cell Res [Internet] 21 (1) (2011) 103–115, https://doi.org/10.1038/cr.2010.178.
[12] B.I. Hudson, A.M. Carter, E. Harja, A.Z. Kalea, M. Arriero, H. Yang, et al., Identification, classification, and expression ofRAGEgene splice variants, FASEB J 22 (5) (2008) 1572–1580, https://doi.org/10.1096/fj.07-9909com [Internet].
[13] W. Rungratanawanich, Y. Qu, X. Wang, M.M. Essa, B.-J. Song, Advanced glycation end products (AGEs) and other adducts in aging-related diseases and alcohol-mediated tissue injury, Exp. Mol. Med. 53 (2) (2021) 168–188, https://doi.org/10.1038/s12276-021-00561-7 [Internet].
[14] S.F. Yan, R. Ramasamy, A.M. Schmidt, The receptor for advanced glycation endproducts (RAGE) and cardiovascular disease, Expert Rev Mol Med [Internet] 11 (e9) (2009), https://doi.org/10.1017/s146239940900101x.
[15] H. Koyama, H. Yamamoto, Y. Nishizawa, RAGE and soluble RAGE: potential therapeutic targets for cardiovascular diseases, Mol Med [Internet] 13 (11–12) (2007) 625–635, https://doi.org/10.2119/2007-00087.koyama.
[16] C. Ott, K. Jacobs, E. Haucke, A. Navarrete Santos, T. Grune, A. Simm, Role of advanced glycation end products in cellular signaling, Redox Biol [Internet] 2 (2014) 411–429, https://doi.org/10.1016/j.redox.2013.12.016.
[17] M.E. Garay-Sevilla, A. Gomez-Ojeda, I. González, C. Luévano-Contreras, A. Rojas, Contribution of RAGE axis activation to the association between metabolic syndrome and cancer, Mol Cell Biochem [Internet] 476 (3) (2021) 1555–1573, https://doi.org/10.1007/s11010-020-04022-z.
[18] H. Unoki, H. Bujo, S.-I. Yamagishi, M. Takeuchi, T. Imaizumi, Y. Saito, Advanced glycation end products attenuate cellular insulin sensitivity by increasing the generation of intracellular reactive oxygen species in adipocytes, Diabetes Res Clin Pract [Internet] 76 (2) (2007) 236–244, https://doi.org/10.1016/j.diabres.2006.09.016.
[19] H. Unoki-Kubota, S.-I. Yamagishi, M. Takeuchi, H. Bujo, Y. Saito, Pyridoxamine, an inhibitor of advanced glycation end product (AGE) formation ameliorates insulin resistance in obese, type 2 diabetic mice, Protein Pept Lett [Internet] 17 (9) (2010) 1177–1181, https://doi.org/10.2174/092986610791760423.
[20] N. Tahara, S.-I. Yamagishi, T. Matsui, M. Takeuchi, Y. Nitta, N. Kodama, et al., Serum levels of AGEs are independent correlates of insulin resistance in nondiabetic subjects, Cardiovasc Ther [Internet] 30 (1) (2012) 42–48, https://doi.org/10.1111/j.1755-5922.2010.00177.x.

[21] J. Rani, I. Mittal, A. Pramanik, N. Singh, N. Dube, S. Sharma, et al., T2DiACoD: a gene atlas of type 2 Diabetes Mellitus associated complex disorders, Sci Rep [Internet] 7 (1) (2017), https://doi.org/10.1038/s41598-017-07238-0.

[22] K. Lian, C. Du, Y. Liu, D. Zhu, W. Yan, H. Zhang, et al., Impaired adiponectin signaling contributes to disturbed catabolism of branched-chain amino acids in diabetic mice, Diabetes 64 (1) (2015) 49–59, https://doi.org/10.2337/db14-0312 [Internet].

[23] Y. Wu, H. Gao, H. Li, Y. Tabara, M. Nakatochi, Y.-F. Chiu, et al., A meta-analysis of genome-wide association studies for adiponectin levels in East Asians identifies a novel locus near WDR11-FGFR2, Hum Mol Genet [Internet] 23 (4) (2014) 1108–1119, https://doi.org/10.1093/hmg/ddt488.

[24] S. Francke, A genome-wide scan for coronary heart disease suggests in Indo-Mauritians a susceptibility locus on chromosome 16p13 and replicates linkage with the metabolic syndrome on 3q27, Hum Mol Genet [Internet] 10 (24) (2001) 2751–2765, https://doi.org/10.1093/hmg/10.24.2751.

[25] A.H. Kissebah, G.E. Sonnenberg, J. Myklebust, M. Goldstein, K. Broman, R.G. James, et al., Quantitative trait loci on chromosomes 3 and 17 influence phenotypes of the metabolic syndrome, Proc Natl Acad Sci U S A [Internet] 97 (26) (2000) 14478–14483, https://doi.org/10.1073/pnas.97.26.14478.

[26] B. Zietz, C. Buechler, K. Kobuch, M. Neumeier, J. Schölmerich, A. Schäffler, Serum levels of adiponectin are associated with diabetic retinopathy and with adiponectin gene mutations in Caucasian patients with diabetes mellitus type 2, Exp. Clin. Endocrinol. Diabetes 116 (9) (2008) 532–536, https://doi.org/10.1055/s-2008-1058086 [Internet].

[27] E.Y. Choe, H.J. Wang, O. Kwon, K.J. Kim, B.S. Kim, B.-W. Lee, et al., Variants of the adiponectin gene and diabetic microvascular complications in patients with type 2 diabetes, Metabolism 62 (5) (2013) 677–685, https://doi.org/10.1016/j.metabol.2012.11.005 [Internet].

[28] S. Del Turco, T. Navarra, A. Gastaldelli, G. Basta, Protective role of adiponectin on endothelial dysfunction induced by AGEs: a clinical and experimental approach, Microvasc Res [Internet] 82 (1) (2011) 73–76, https://doi.org/10.1016/j.mvr.2011.03.003.

[29] K. Ishikawa, S. Yoshida, Y. Kobayashi, Y. Zhou, T. Nakama, S. Nakao, et al., Microarray analysis of gene expression in fibrovascular membranes excised from patients with proliferative diabetic retinopathy, Invest Ophthalmol Vis Sci [Internet] 56 (2) (2015) 932–946, https://doi.org/10.1167/iovs.14-15589.

[30] M.E. Ritchie, B. Phipson, D. Wu, Y. Hu, C.W. Law, W. Shi, et al., Limma powers differential expression analyses for RNA-sequencing and microarray studies, Nucleic Acids Res [Internet] 43 (7) (2015), https://doi.org/10.1093/nar/gkv007 e47–e47.

[31] M. Ashburner, C.A. Ball, J.A. Blake, D. Botstein, H. Butler, J.M. Cherry, et al., Gene Ontology: tool for the unification of biology, Nat Genet [Internet] 25 (1) (2000) 25–29, https://doi.org/10.1038/75556.

[32] M. Kanehisa, KEGG: Kyoto encyclopedia of genes and genomes, Nucleic Acids Res [Internet] 28 (1) (2000) 27–30, https://doi.org/10.1093/nar/28.1.27.

[33] M. Kanehisa, M. Furumichi, Y. Sato, M. Ishiguro-Watanabe, M. Tanabe, KEGG: integrating viruses and cellular organisms, Nucleic Acids Res [Internet] 49 (D1) (2021) D545–D551, https://doi.org/10.1093/nar/gkaa970.

[34] A. Subramanian, P. Tamayo, V.K. Mootha, S. Mukherjee, B.L. Ebert, M.A. Gillette, et al., Gene set enrichment analysis: a knowledge-based approach for interpreting genome-wide expression profiles, Proc Natl Acad Sci U S A [Internet] 102 (43) (2005) 15545–15550, https://doi.org/10.1073/pnas.0506580102.

[35] D. Szklarczyk, A.L. Gable, D. Lyon, A. Junge, S. Wyder, J. Huerta-Cepas, et al., STRING v11: protein–protein association networks with increased coverage, supporting functional discovery in genome-wide experimental datasets, Nucleic Acids Res [Internet] 47 (D1) (2019) D607–D613, https://doi.org/10.1093/nar/gky1131.

[36] P. Shannon, A. Markiel, O. Ozier, N.S. Baliga, J.T. Wang, D. Ramage, et al., Cytoscape: a software environment for integrated models of biomolecular interaction networks, Genome Res [Internet] 13 (11) (2003) 2498–2504, https://doi.org/10.1101/gr.1239303.

[37] G.D. Bader, C.W.V. Hogue, An automated method for finding molecular complexes in large protein interaction networks, BMC Bioinf. 4 (1) (2003), https://doi.org/10.1186/1471-2105-4-2 [Internet].

[38] C.-H. Chin, S.-H. Chen, H.-H. Wu, C.-W. Ho, M.-T. Ko, C.-Y. Lin, cytoHubba: identifying hub objects and sub-networks from complex interactome, BMC Syst Biol [Internet] 8 (S4) (2014), https://doi.org/10.1186/1752-0509-8-s4-s11.

[39] D. Warde-Farley, S.L. Donaldson, O. Comes, K. Zuberi, R. Badrawi, P. Chao, et al., The GeneMANIA prediction server: biological network integration for gene prioritization and predicting gene function, Nucleic Acids Res [Internet] 38 (suppl_2) (2010) W214–W220, https://doi.org/10.1093/nar/gkq537.

[40] E. Becht, N.A. Giraldo, L. Lacroix, B. Buttard, N. Elarouci, F. Petitprez, et al., Erratum to: estimating the population abundance of tissue-infiltrating immune and stromal cell populations using gene expression, Genome Biol [Internet] 17 (1) (2016), https://doi.org/10.1186/s13059-016-1113-y.

[41] D.W.I.I. Parke, The American academy of ophthalmology and the formation of the American board of ophthalmology, Ophthalmology 123 (9) (2016) S12–S14, https://doi.org/10.1016/j.ophtha.2016.06.009 [Internet].

[42] T. Kadowaki, Adiponectin and adiponectin receptors in insulin resistance, diabetes, and the metabolic syndrome, J Clin Invest [Internet] 116 (7) (2006) 1784–1792, https://doi.org/10.1172/jci29126.

[43] J.H. Stern, J.M. Rutkowski, P.E. Scherer, Adiponectin, Leptin, and fatty acids in the maintenance of metabolic homeostasis through adipose tissue crosstalk, Cell Metab [Internet] 23 (5) (2016) 770–784, https://doi.org/10.1016/j.cmet.2016.04.011.

[44] M. Takahashi, Y. Arita, K. Yamagata, Y. Matsukawa, K. Okutomi, M. Horie, et al., Genomic structure and mutations in adipose-specific gene, adiponectin, Int J Obes (Lond) [Internet] 24 (7) (2000) 861–868, https://doi.org/10.1038/sj.ijo.0801244.

[45] T.-A. Sakaue, Y. Fujishima, Y. Fukushima, Y. Tsugawa-Shimizu, S. Fukuda, S. Kita, et al., Adiponectin accumulation in the retinal vascular endothelium and its possible role in preventing early diabetic microvascular damage, Sci Rep [Internet] 12 (1) (2022), https://doi.org/10.1038/s41598-022-08041-2.

[46] A. Achari, S. Jain, Adiponectin, a therapeutic target for obesity, diabetes, and endothelial dysfunction, Int J Mol Sci [Internet] 18 (6) (2017) 1321, https://doi.org/10.3390/ijms18061321.

[47] T. Yamauchi, J. Kamon, Y. Minokoshi, Y. Ito, H. Waki, S. Uchida, et al., Adiponectin stimulates glucose utilization and fatty-acid oxidation by activating AMP-activated protein kinase, Nat Med [Internet] 8 (11) (2002) 1288–1295, https://doi.org/10.1038/nm788.

[48] T. Yamauchi, J. Kamon, Y. Ito, A. Tsuchida, T. Yokomizo, S. Kita, et al., Cloning of adiponectin receptors that mediate antidiabetic metabolic effects, Nature 423 (6941) (2003) 762–769, https://doi.org/10.1038/nature01705 [Internet].

[49] T. Lin, Y. Qiu, Y. Liu, R. Mohan, Q. Li, B. Lei, Expression of adiponectin and its receptors in type 1 diabetes mellitus in human and mouse retinas, Mol. Vis. 19 (2013) 1769–1778.

[50] T. Matsunami, Y. Sato, S. Ariga, T. Sato, H. Kashimura, Y. Hasegawa, et al., Regulation of oxidative stress and inflammation by hepatic adiponectin receptor 2 in an animal model of nonalcoholic steatohepatitis, Int. J. Clin. Exp. Pathol. 3 (5) (2010) 472–481.

[51] P. Thomas, Membrane progesterone receptors (mPRs, PAQRs): review of structural and signaling characteristics, Cells 11 (11) (2022) 1785, https://doi.org/10.3390/cells11111785 [Internet].

[52] J. Ye, M. Gao, X. Guo, H. Zhang, F. Jiang, Breviscapine suppresses the growth and metastasis of prostate cancer through regulating PAQR4-mediated PI3K/Akt pathway, Biomed Pharmacother [Internet] 127 (110223) (2020) 110223, https://doi.org/10.1016/j.biopha.2020.110223.

[53] Y.T. Tang, T. Hu, M. Arterburn, B. Boyle, J.M. Bright, P.C. Emtage, et al., PAQR proteins: a novel membrane receptor family defined by an Ancient7-transmembrane pass motif, J Mol Evol [Internet] 61 (3) (2005) 372–380, https://doi.org/10.1007/s00239-004-0375-2.

[54] L.F. Castelnovo, L. Caffino, V. Bonalume, F. Fumagalli, P. Thomas, V. Magnaghi, Membrane progesterone receptors (mPRs/PAQRs) differently regulate migration, proliferation, and differentiation in rat Schwann cells, J Mol Neurosci [Internet] 70 (3) (2020) 433–448, https://doi.org/10.1007/s12031-019-01433-6.

[55] S. Ricard-Blum, The collagen family, Cold Spring Harb Perspect Biol [Internet] 3 (1) (2011), https://doi.org/10.1101/cshperspect.a004978 a004978–a004978.

[56] D. Sergi, H. Boulestin, F.M. Campbell, L.M. Williams, The role of dietary advanced glycation end products in metabolic dysfunction, Mol Nutr Food Res [Internet] 65 (1) (2021), https://doi.org/10.1002/mnfr.201900934.

[57] Y. Takayanagi, M. Yamanaka, J. Fujihara, Y. Matsuoka, Y. Gohto, A. Obana, et al., Evaluation of relevance between advanced glycation end products and diabetic retinopathy stages using skin autofluorescence, Antioxidants (Basel) [Internet] 9 (11) (2020) 1100, https://doi.org/10.3390/antiox9111100.

[58] L. Chen, Y. Cui, B. Li, J. Weng, W. Wang, S. Zhang, et al., Advanced glycation end products induce immature angiogenesis in in vivo and ex vivo mouse models, Am J Physiol Heart Circ Physiol [Internet] 318 (3) (2020) H519–H533, https://doi.org/10.1152/ajpheart.00473.2019.

[59] C.M. McVicar, M. Ward, L.M. Colhoun, J. Guduric-Fuchs, A. Bierhaus, T. Fleming, et al., Role of the receptor for advanced glycation endproducts (RAGE) in retinal vasodegenerative pathology during diabetes in mice, Diabetologia 58 (5) (2015) 1129–1137, https://doi.org/10.1007/s00125-015-3523-x [Internet].

[60] K. Palanisamy, R.N. Nareshkumar, S. Sivagurunathan, R. Raman, K.N. Sulochana, S. Chidambaram, Anti-angiogenic effect of adiponectin in human primary microvascular and macrovascular endothelial cells, Microvasc Res [Internet] 122 (2019) 136–145, https://doi.org/10.1016/j.mvr.2018.08.002.
[61] A.M. Abu El-Asrar, A. Ahmad, M.M. Siddiquei, A. De Zutter, E. Allegaert, P.W. Gikandi, et al., The proinflammatory and proangiogenic macrophage migration inhibitory factor is a potential regulator in proliferative diabetic retinopathy, Front Immunol [Internet] 10 (2019), https://doi.org/10.3389/fimmu.2019.02752.
[62] Y. Mizukami, J. Li, X. Zhang, M.A. Zimmer, O. Iliopoulos, D.C. Chung, Hypoxia-inducible factor-1-independent regulation of vascular endothelial growth factor by hypoxia in colon cancer, Cancer Res [Internet] 64 (5) (2004) 1765–1772, https://doi.org/10.1158/0008-5472.can-03-3017.
[63] H. Zong, M. Ward, A. Madden, P.H. Yong, G.A. Limb, T.M. Curtis, et al., Hyperglycaemia-induced pro-inflammatory responses by retinal Müller glia are regulated by the receptor for advanced glycation end-products (RAGE), Diabetologia 53 (12) (2010) 2656–2666, https://doi.org/10.1007/s00125-010-1900-z [Internet].
[64] J.R. Dauch, D.E. Bender, L.A. Luna-Wong, W. Hsieh, B.M. Yanik, Z.A. Kelly, et al., Neurogenic factor-induced Langerhans cell activation in diabetic mice with mechanical allodynia, J. Neuroinflammation 10 (1) (2013), https://doi.org/10.1186/1742-2094-10-64 [Internet].
[65] J.K. Juranek, M.S. Geddis, F. Song, J. Zhang, J. Garcia, R. Rosario, et al., RAGE deficiency improves postinjury sciatic nerve regeneration in type 1 diabetic mice, Diabetes 62 (3) (2013) 931–943, https://doi.org/10.2337/db12-0632 [Internet].
[66] A.W. Stitt, AGEs and diabetic retinopathy, Invest Ophthalmol Vis Sci [Internet] 51 (10) (2010) 4867, https://doi.org/10.1167/iovs.10-5881.